VIBRATION POWER GENERATION WITH PIEZOELECTRIC ELEMENT USING MECHANICAL-ACOUSTIC COUPLING IN ACTUAL ENVIRONMENT

B.Eng. Ohba Y.[1], and Prof. D.Eng. Moriyama H.[2]
Course of Mechanical Engineering, Graduate School of Tokai University, Japan [1]
Department of Prime Mover Engineering, Tokai University, Japan [2]

6bemm001@u-tokai.ac.jp

Abstract: *This paper describes electricity generation characteristics of the vibration power generator with piezoelectric elements. In general, it is well-known that the above generator has low generation efficiency, having so simple structure. Moreover, vibrations of broad frequency band, which exist in actual environment, bring the characteristics to lower efficiency in comparison with the particular situation in which the host structure is excited by the vibration of the natural frequency. In this study, the vibrations of broad frequency band, i.e. random vibration, attracts attention and mechanical-acoustic coupling with an internal sound field enclosed by the host structures, on which the piezoelectric element is installed, is adopted to improve the electricity generation efficiency. The behavior of mechanical-acoustic coupling is determined by the relationship between the respective characteristics of the host structure vibrations and the internal sound field, so that the electricity generation efficiency depends strongly on those dimensions. Here, the electric power and the electricity generation efficiency are regarded as the representative characteristics of the electricity generation, then the characteristics are considered based on them with changing the dimensions to find the condition in which the efficiency can be improved. As a result, the applicability of such a power generation system in actual environments is mentioned.*

Keywords: MECHANICAL-ACOUSTIC COUPLING, CYLINDRICAL STRUCTURE, THIN END PLATE, INTERNAL SOUND FIELD, PLATE VIBRATION, NATURAL FREQENCY, RANDOM EXCITATION, PIEZOELECTRIC ELEMENT

1. Introduction

Scavenging untapped vibration energy and converting it into usable electric energy via piezoelectric materials has attracted considerable attention and has been regarded as one of new energy sources[1]. The authors have also been interested in a mechanical-acoustic coupling problem. The representative example was investigated as an architectural acoustic problem via a coupled panel-cavity system consisting of a rectangular box with slightly absorbing walls and a simply supported panel. The effect of the panel characteristics on the decay behavior of the sound field in the cavity was considered both theoretically and experimentally[1,2].

To develop a new electricity generation system, we adopt a cylindrical structure with plates at both ends as an analytical model, because the vibration area of the model on which piezoelectric elements can be installed is twice as large as that in the case of a single plate. The plate vibration induces electricity generation via electro-mechanical coupling with the piezoelectric effect of the surface-mounted piezoelectric element, while the plate vibration of the excitation side oscillates the other plate via mechanical-acoustic coupling. Consequently, the electro-mechanical-acoustic coupling problem must be considered and not only the natural frequency of the plate is adopted as the excitation frequency, but also the excitation of broad frequency band, i.e. random excitation, is attempted to assume an actual environment.

2. Analytical method

2.1 Analytical model

The analytical model consists of a cavity with two circular end plates, as shown in Fig. 1. Plates 1 and 2 are supported by translational and rotational springs distributed at constant intervals and the support conditions are determined by the translational spring stiffnesses T_1, T_2 and the rotational spring stiffnesses R_1, R_2, and then the suffixes 1 and 2 indicate plates 1 and 2, respectively. The plates of radius r_c have a Young's modulus E_c and a Poisson's ratio ν_c, however, the plate thickness is denoted by h_{c1} and h_{c2}, because it's possible the plates are different in the thickness. On the surfaces of both plates, piezoelectric elements are installed at the centers of the plates and have radius r_p, thickness h_p, Young's modulus E_p, and Poisson's ratio ν_p. Then an electrode plate is sandwiched between the above plate and piezoelectric element and has radius r_b, thickness h_b, Young's modulus E_b, and Poisson's ratio ν_b. The suffixes *c*, *p*, and *b* herein indicate the circular plate, piezoelectric element and electrode plate. On the other hand, the sound field, which is assumed to be cylindrical, has the same radius as that of the plates and varying length L because the resonance frequency depends on the length. The boundary conditions are considered structurally and acoustically rigid at the lateral wall between the structure and sound field. The coordinates used are radius r, angle ϕ between the planes of the plates and the cross-sectional plane of the cavity and distance z along the cylinder axis. The periodic point force F is applied to plate 1 at distance r_1 and angle ϕ_1. The natural frequency of the plates is employed as the excitation frequency.

w_{c1} and w_{c2} are the flexural displacements of plates 1 and 2, and w_{p1} and w_{p2} are those of the piezoelectric elements installed on the plates. They are found by substituting X^{s}_{cnm} of Equation (2) for the plate modes into Equation (1) as suitable trial functions. The flexural displacements of the piezoelectric elements are identical to those of the plates, respectively, because it is assumed that the piezoelectric elements adhere completely to each circular plate through the electrode plate.

$$w_{c1} = w_{p1} = \sum_{s=0}^{1}\sum_{n=0}^{\infty}\sum_{m=0}^{\infty} X^{s}_{nm} A^{s}_{1nm} \mathrm{e}^{\mathrm{j}(\omega t+\alpha_1)}, \quad (1)$$

$$w_{c2} = w_{p2} = \sum_{s=0}^{1}\sum_{n=0}^{\infty}\sum_{m=0}^{\infty} X^{s}_{nm} A^{s}_{2nm} \mathrm{e}^{\mathrm{j}(\omega t+\alpha_2)},$$

$$X^{s}_{nm} = \sin(n\phi + s\pi/2)(r/r_c)^m, \quad (2)$$

Where n, m, and s are, respectively, the circumferential order, radial order, and symmetry index with respect to the plate vibration. A^{s}_{1nm} and A^{s}_{2nm} are coefficients to be determined, ω is the angular frequency of the harmonic point force acting on the plate, and t is the elapsed time. α_1 and α_2 are the phases of the respective plate vibrations. In this analysis, α_1 is set to 0°, and α_2 ranges from 0° to 180°.

2.2 Modelling of Piezoelectric Part

Only the piezoelectric part of plate 1 is used to explain its modelling in this section. The relationships of stress σ_{p1}, strain ε_{p1}, electric displacement D_1, and electric field E_1 are as follows:

$$\begin{Bmatrix}\sigma_{p1}\\ D_1\end{Bmatrix} = \begin{bmatrix}E^{E}_{p} & -e^{T}\\ e & \gamma^{\varepsilon}\end{bmatrix}\begin{Bmatrix}\varepsilon_{p1}\\ E_1\end{Bmatrix}. \quad (3)$$

E^{E}_{p} signifies Young's modulus that was measured at a constant electric field, and γ^{ε} indicates the dielectric constant that was measured at a constant strain. The above equation expresses

relationships between electrical and mechanical characteristics of a piezoelectric element, and the stress is concretely related to the electric field by the piezoelectric coupling coefficient *e*. The piezoelectric coupling coefficient is expressed as

$$e = d_{31} E_p^E, \tag{4}$$

where d_{31} is the piezoelectric strain constant, in which the electric field occurs in the normal direction of the in-plane strain.

Then the electric field E_1, which occurs between both sides of the piezoelectric element, is expressed as follows:

$$E_1 = Y_{nm} v_1 = -R_p \dot{q}_1 = \mathrm{j}\omega B_{1nm}^s \mathrm{e}^{\mathrm{j}(\omega t+\alpha_1)}. \tag{5}$$

v_1 is the voltage that occurs in the electric field. We assume that the electric potential across the piezoelectric element is constant, since it is in the field that is not applied to the plate. Thus, Y_{nm} is defined as described above. R_p is the overall resistance value in an electricity generation circuit. The magnitude of the electric charge q_1 depends on the coefficient B_{1nm}^s that is determined in this analysis as well as A_{1nm}^s.

$$Y_{nm} = \begin{cases} -1/h_p & h_c/2 + h_b < z < h_c/2 + h_b + h_p, \\ 0 & -h_c/2 < z < h_c/2 + h_b, \end{cases} \tag{6}$$

$$q_1 = B_{1nm}^s \mathrm{e}^{\mathrm{j}(\omega t+\alpha_1)}. \tag{7}$$

In order to easily express the electro-mechanical equation, the elements $M_{p1nmm'}^s$ and $K_{p1nmm'}^s$ of the mass and stiffness matrices can be denoted as

$$M_{p1nmm'}^s = \int_{V_{p1}} \rho_p X_{nm}^s X_{nm'}^s \mathrm{d}V_{p1}, \tag{8}$$

$$K_{p1nmm'}^s = \int_{V_{p1}} z^2 X_{nm}^{s\,''} E_p^E X_{nm'}^{s\,''} \mathrm{d}V_{p1}. \tag{9}$$

The index *m'* is also of a radial order and has a transposed relation to *m*. The elements θ_1 and C_{p1} of the electro-mechanical coupling and capacitance matrices are defined as

$$\theta_1 = -\int_{V_{p1}} z\rho_p X_{nm}^s e Y_{nm'} \mathrm{d}V_{p1}, \tag{10}$$

$$C_{p1} = \int_{V_{p1}} Y_{nm} \gamma^{\varepsilon} Y_{nm'} \mathrm{d}V_{p1}. \tag{11}$$

2.3 Governing equations of electro-mechanical-acoustic coupling

Here, electro-mechanical coupling is considered from the above several relationships, and then mechanical-acoustic coupling is also taken based on the relationships between the vibrations of both plates and the sound field into the cylindrical enclosure. As a result, this electricity generation phenomenon depends strongly on electro-mechanical-acoustic coupling, so that the motions of both plates having a piezoelectric part are governed by the following Eqs. (12) and (13), respectively:

$$\sum_{m=0}^{\infty}\Big[\Big\{K_{c1nmm'}^s(1+\mathrm{j}\eta_c)+K_{p1nmm'}^s(1+\mathrm{j}\eta_p)+K_{b1nmm'}^s(1+\mathrm{j}\eta_b) - \omega^2\left(M_{c1nmm'}^s+M_{p1nmm'}^s+M_{b1nmm'}^s\right)\Big\}+r_c F_{sn}\left\{T+\left(\frac{m}{r_c}\right)\times\left(\frac{m'}{r_c}\right)R\right\}\Big]A_{1nm'}^s \mathrm{e}^{\mathrm{j}\alpha_1} - \sum_{m'=0}^{\infty}\theta_1 v B_{1nm'}^s \mathrm{e}^{\mathrm{j}\alpha_1} = \mathbf{F}_{nm}^s \mathrm{e}^{\mathrm{j}\alpha_1} - \mathbf{S}_{1nm}^s \tag{12}$$

$$\sum_{m=0}^{\infty}\Big[\Big\{K_{c2nmm'}^s(1+\mathrm{j}\eta_c)+K_{p2nmm'}^s(1+\mathrm{j}\eta_p)+K_{b2nmm'}^s(1+\mathrm{j}\eta_b) - \omega^2\left(M_{c2nmm'}^s+M_{p2nmm'}^s+M_{b2nmm'}^s\right)\Big\}+r_c F_{sn}\left\{T+\left(\frac{m}{r_c}\right)\times\left(\frac{m'}{r_c}\right)R\right\}\Big]A_{2nm'}^s \mathrm{e}^{\mathrm{j}\alpha_2} - \sum_{m'=0}^{\infty}\theta_2 v B_{2nm'}^s \mathrm{e}^{\mathrm{j}\alpha_2} = \mathbf{S}_{2nm}^s \tag{13}$$

$K_{c1nmm'}^s$, K_{b1nmm}^s, and $K_{c2nmm'}^s$, $K_{b2nmm'}^s$ are stiffness matrix elements and $M_{c1nmm'}^s$, M_{b1nmm}^s, and $M_{c2nmm'}^s$, $M_{b2nmm'}^s$ are mass matrix elements with respect to the circular and electrode plates, respectively. These are elements of the symmetrical matrices, because the index *m'* has a transposed relation to *m*, as well as $M_{p1nmm'}^s$ and $K_{p1nmm'}^s$. η_c, η_p, and η_b are the structural damping factors of the circular plate, piezoelectric element and electrode plate, respectively. Moreover, F_{sn} is a coefficient that is determined by the indices *n* and *s*, $\mathbf{F}_{nm}^s$ is a load vector that expresses the point force on plate 1, and $\mathbf{S}_{nm1}^s$ and $\mathbf{S}_{nm2}^s$ are the acoustic excitation vectors that express the acoustic excitations of both plates. The details of F_{sn} and the elements F_{nm}^s, S_{nm1}^s, and S_{nm2}^s of the respective vectors are as follows:

$$F_{sn} = \begin{cases} \pi, \text{ at } n \neq 0, \\ 0, \text{ at } n = 0 \text{ and } s = 0, \\ 2\pi, \text{ at } n = 0 \text{ and } s = 1, \end{cases} \tag{14}$$

$$F_{nm}^s = \int_{A_1} F\delta(r-r_1)\delta(\phi-\phi_1) X_{nm}^s \mathrm{d}A_1, \tag{15}$$

$$S_{1nm}^s = \int_{A_1} P_s X_{nm}^s \mathrm{d}A_1, \quad S_{2nm}^s = \int_{A_2} P_s X_{nm}^s \mathrm{d}A_2. \tag{16}$$

Here, δ is the delta function associated with the point force on plate 1, whose area is denoted by A_1. P_s is the sound pressure at an arbitrary point on the boundary surface of the plates, and A_2 signifies the area of plate 2.

On the other hand, the electricity generation behaviors of these piezoelectric elements are governed by the following Eqs. (17) and (18), respectively:

$$\sum_{m'=0}^{\infty} C_{p1}^{-1}\theta_1 A_{1nm'}^s = \sum_{m'=0}^{\infty}\left(\mathrm{j}\omega R_p + C_{p1}^{-1}\right)B_{1nm'}^s, \tag{17}$$

$$\sum_{m'=0}^{\infty} C_{p2}^{-1}\theta_2 A_{2nm'}^s = \sum_{m'=0}^{\infty}\left(\mathrm{j}\omega R_p + C_{p2}^{-1}\right)B_{2nm'}^s. \tag{18}$$

3. Experimental apparatus and method

Figures 2 shows the configuration of the experimental apparatus used in this study. The structure consists of a steel cylinder with circular aluminum end plates whose radius r_c and thickness h_c are 153 mm and 3.0 mm, respectively. The cylinder has the same inner radius as the radius of the end plate and the length *L* can range from 500 to 2000 mm to emulate the analytical model. Plate 1 is subjected to the point force excited by a small vibrator.

The cylinder has the same inner radius as the radius of the end plate and the length *L* can range from 500 to 2000 mm to emulate the analytical model. Plate 1 is subjected to the point force excited by a small vibrator.

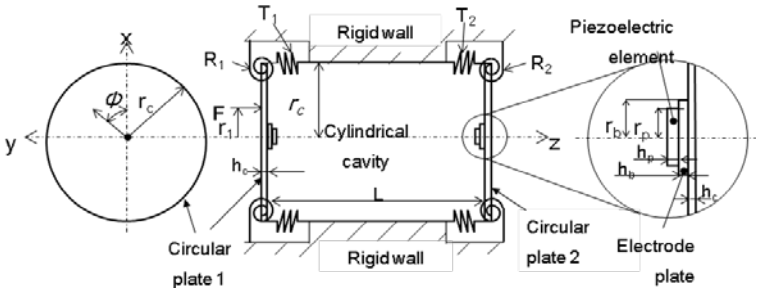

***Fig. 1** Configuration of analytical model.*

Plate 1 is subjected to the point force excited by a small vibrator. The cylinder has the same inner radius as the radius of the end plate and the length L can range from 500 to 2000 mm to emulate the analytical model. Plate 1 is subjected to the point force excited by a small vibrator. The excitation is carried out near the natural frequency of the (0,0) mode, otherwise it covers the wide frequency range due to assuming actual situations and signifies the random excitation. The position of the point force r_1 is normalized by radius r_c and is set to $r_1/ r_c = 0.4$.

To estimate the mechanical power P_m supplied to plate 1 by the small vibrator, an acceleration sensor is installed near the position of the point force on plate 1, and P_m is predicted from the point force and acceleration a_1. The phase difference between the plate vibrations is also measured owing to the installation of the acceleration sensor at the same position on plate 2, resulting in significant effects on the mechanical-acoustic coupling. To estimate the internal acoustic characteristics, the sound pressure level in the cavity is measured using condenser microphones with a probe tube. The tips of the probe tubes are located near the plates and the cylinder wall, which are the approximate locations of the maximum sound pressure level when the sound field becomes resonant.

The piezoelectric elements are installed at the centers of both plates. The electric power P_{e1} and P_{e2} generated by the expansion and contraction of the piezoelectric elements on plates 1 and 2 are discharged through the resistance circuit, which consists of three resistors having resistances R_v, R_i, and R_c, as shown in Figure 2. To grasp the effect of mechanical-acoustic coupling on energy harvesting, the electric power and other data are also measured without the cylinder (i.e. in the electricity generation under the vibration of only plate 1) and are estimated in comparison with those with cylinder. In such an estimation, electricity generation efficiency is used and is derived from the electric power normalized by the mechanical power P_m supplied to plate 1 by the vibrator. However, the electricity generation efficiencies, which are obtained from P_{e1}, P_{e2}, and their total electric power P_e, are denoted by P_{em1}, P_{em2}, and P_{em}, respectively, when electro-mechanical coupling is taken into consideration.

3. Results and discussion

3.1 Electricity generation characteristics in natural frequency excitation

Here, the thickness of plates is set to $h_c = 3$ mm in Figs. 1and 2. The support condition of plates, which have flexural rigidity D [$= E_c h_c^3/\{12(1-\nu_c^2)\}$], is expressed by the nondimensional stiffness parameters T_{n1} ($= T_{c1} r_c^3/D$) , T_{n2}, R_{n1} ($= R_{c1} r_c/D$), and R_{n2}. If R_{n1} and R_{n2} range from 0 to 10^8 when T_{n1} and T_{n2} are 10^8, the support condition can be assumed, from a simple support to a clamped support.

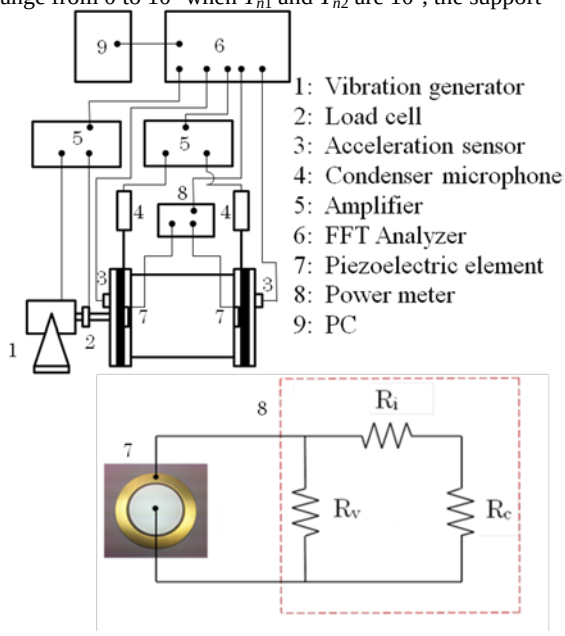

Fig. 2 Experimental apparatus.

Figure 3 shows the sound pressure level L_{pv}, which is averaged over the entire volume of the cavity and is maximized at each L when the phase α_2 ranges from 0 to 180°, as functions of L.

The excitation frequency f is 280 Hz, because both plates have the $h_c = 3$ mm and are supported by $T_{n1} = T_{n2} = 10^8$ and $R_{n1} = R_{n2} = 10$ to get closer to the apparatus. The theoretical level L_{pv} peaks at 610, 1230, and 1840 mm.

The peaks are caused by the promotion of mechanical-acoustic coupling between the plate vibration and acoustic modes. Then the acoustic modes are the (0,0,1), (0,0,2), and (0,0,3) modes whose plane modal shape is similar to that of plate vibration mode (0,0). To validate these theoretical results, the sound pressure levels L_{p1} and L_{p2}, which are measured near plates 1 and 2, are also indicated. The experimental peaks occur around the lengths where L_{pv} peaks, whereas L_{p1} decreases remarkably around L = 950 and 1600 mm in the process of shifting acoustic modes because of a changing L.

Figure 4 shows the electricity generation efficiency P_{em} as functions of f under the vibration of only plate and the vibrations of plates 1 and 2 with mechanical-acoustic coupling. However, P_{em} with coupling corresponds to the maximum electric power P_e at each f where L and α_2 are changed. Although both values of P_{em} have peaks in the vicinity of 280 Hz and exceed 7 %, P_{em} with coupling is somewhat improved in comparison with that without coupling. With respect to the electricity generation with coupling, $R_{n1} = 10^{0.78}$ is also adopted instead of $R_{n1} = 10$ to make the support condition approximate to the actual situation. Because plate 1 receives the additional mass of the stick exciting it, its natural frequency is shifted to a lower frequency region than the above cases. As a result, P_{em} peaks in the vicinity of 270 Hz and is suppressed until around 6%.

Figure 5 shows variations in the experimental P_{em} with changing L. Since the natural frequency of plate 1 is shifted in the lower region by the effect of the additional mass, as described above, the excitation frequencies f = 256 and 270 Hz are adopted and are close to the respective natural frequencies of plates 1 and 2. P_{em} at f = 270 Hz peaks at approximately L = 600, 1220, and 1870 mm and is similar to L_{p1} and L_{p2} in Fig. 3 in the length where the peaks appear.

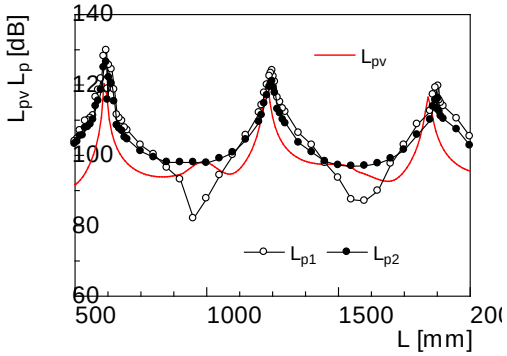

***Fig. 3** Sound pressure level inside cavity as function of cylinder length.*

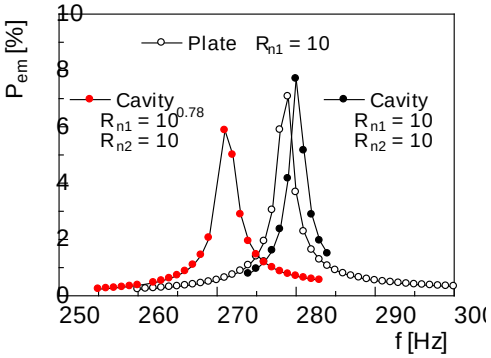

***Fig. 4** Electricity generation efficiency as function of excitation frequency.*

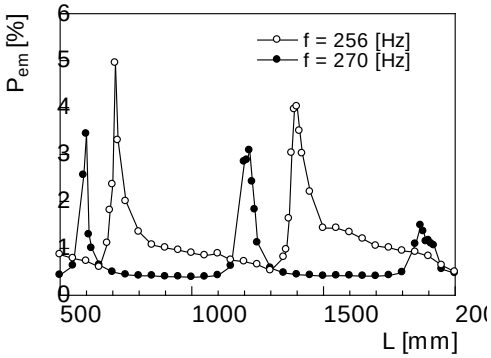

Fig. 5 *Electricity generation efficiency as function of cylinder length.*

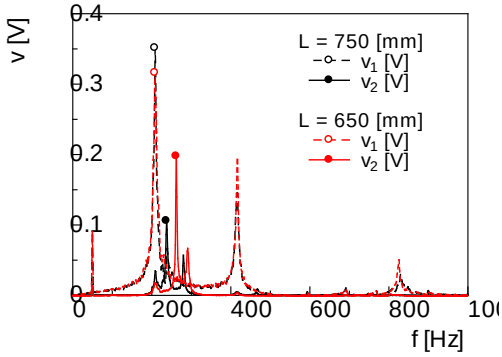

Fig. 6 *Voltage characteristics in random excitation.*

This excitation frequency is adjusted to be close to the natural frequency of plate 2 and is different from that of plate 1, so that the vibration of plate 1, which is subjected to the point force, is suppressed. However, because plate 2 is excited acoustically by the internal sound field via mechanical-acoustic coupling, P_{em} increases rapidly at the above lengths where the coupling is promoted. The electric power P_{e2} of plate 2 contributes almost to P_{em}, hence this is regarded as the electricity generation controlled by the vibration of plate 2.

In the case of f = 256 Hz, since the excitation frequency is close to the natural frequency of plate 1, the coupling is promoted between the vibration of plate 1 and the sound field, weakened between the vibration of plate 2. As described above, under a constraint of the experimental apparatus, the load cell cannot be directly installed on plate 1, so that the point force is applied to plate 1 via a stick from the vibration generator.

Therefore, an additional mass derived from the stick contributes to shift the natural frequency to the lower frequency region, not avoided in this experiment. Then such a tendency lowering the natural frequency brings the appearance of P_{em} peaks to the longer lengths. P_{em} peaks at both excitation frequencies are caused by the promotion of coupling with the (0,0,1), (0,0,2), and (0,0,3) modes, being different in those derivations.

P_{em} values decrease with increasing L and are maximized at the respective first peaks, i.e. by the coupling with the (0,0,1) mode. Those values are smaller than the theoretical results, as shown in Fig. 4. In the actual situation, the reverse sides of the plate surfaces facing to the internal sound field are bounded with atmosphere and the acoustic radiations should also take place on them. In the theoretical procedure, because the interaction between the plate and the medium is not taken into account on such a reverse surface, it is assumed as if the surface is exposed to a vacuum. In other words, it may be considered that the theoretical P_{em} is slightly overestimated. On the other hand, it is confirmed that the experimental P_{em} is suppressed until around 1.7 % without the coupling, i.e. only the plate vibration, in this electricity generation experiment and is much less than the theoretical P_{em} , as shown in Fig. 4. The above interaction is no longer taken into account in this theoretical procedure, so that it is considered that the effect becomes remarkable.

3.2 Electricity generation characteristics in random excitation

Figure 6 shows the voltages v_1 and v_2 based on the respective electricity generations of plates 1 and 2 as functions of the excitation frequency f, which is in the range of 0 Hz to 1000 Hz as the random excitation. Then the cylinder length is set to L = 650 and 750 mm. The variations in v_1 are characterized by the specific peaks, complicated by the random excitation, and are hardly different in changing L. The maximum peaks have the possibility deriving from the (0,0) mode, because of taking place in the vicinity of the natural frequency, as described in the previous section. However, the (0,0) mode cannot be confirm at the peak frequency from the experimental modal analysis and the difference from the natural frequency not affected by the additional mass is expanded in comparison with the difference shown in the previous section. Therefore, the coupling between the plate vibration and the internal sound field is weakened extremely and cannot transfer enough energy to plate 2. However, although v_1 decreases with shifting f to a higher frequency region, the modal shape is formed with shifting f. Consequently, v_2 increases due to the promotion of the coupling with getting closer to the natural frequency of plate 2.

In this case, the resonance frequency of the sound field at L = 650 mm is closer to the natural frequency of plate 2 than that at L = 750 mm, so that v_2 at L = 650 mm exceeds greatly that at L = 750 mm.

In the case of the random excitation, P_{em} slightly exceeds 0.1 % with the coupling, being much less than it without the coupling. Although it is hard to apply practically this system for now, we expect that the performance of energy harvesting is improved by controlling and adjusting plate vibration characteristics.

4. Conclusion

In this study, a new electricity generation system, which consisted of a cylinder with circular end plates on which a piezoelectric element was installed at the center, was proposed. One end plate was excited by the point force, and then not only the natural frequency of the plate was adopted as the excitation frequency, but also the excitation of broad frequency band, i.e. random excitation, was attempted to assume an actual environment.

The mechanical-acoustic coupling between the plate vibrations and the internal sound field is promoted by exciting at the natural frequency of the plate and by setting the cylinder to a specific length. It is verified that the electricity generation efficiency is considerably improved by using the promoted coupling in comparison with that of only the plate vibration without the coupling. Moreover, with respect to the random excitation, the prospect for the improvement of electricity generation characteristics is exhibited by applying the coupling effect to this system.

References

1 Anton S.R. and Sodano H.A., *Smart Materials and Structures*, Vol. 16, No. 3(2007), pp. 1-21.

2 Pan J. and Bies D.A., *J. Acoust. Soc. Am.*,Vol. 87, No.2(1990), pp.691-707.

3 Pan J. and Bies D.A., *J. Acoust. Soc. Am.*, Vol.87, No.2(1990), pp.708-717.